A simplified positron elastic scattering model for Monte Carlo calculations

2006 J. Phys.: Condens. Matter 18 10303

(http://iopscience.iop.org/0953-8984/18/45/016)

INSTITUTE OF PHYSICS PUBLISHING JOURNAL OF PHYSICS: CONDENSED MATTER

J. Phys.: Condens. Matter **18** (2006) 10303–10312 doi:10.1088/0953-8984/18/45/016

A simplified positron elastic scattering model for Monte Carlo calculations

Zine-El-Abidine Chaoui

Laboratory of Optoelectronics and Devices, UFA Setif (19000), Algeria

E-mail: z_chaoui@yahoo.fr

Received 11 May 2006, in final form 6 September 2006
Published 27 October 2006
Online at stacks.iop.org/JPhysCM/18/10303

Abstract

The simplified positron elastic scattering model presented in this paper is a practical method for simulating the positron elastic process. The model yields a simple analytical formula for the random sampling of the angular deflection, which allows fast calculations of the transport of charged particles in matter, and avoids the problem of the infeasibility of detailed simulations when the energy increases up to hundreds of keV. In order to test our modelling, a simple detailed Monte Carlo code has been used to calculate the backscattering probabilities in the keV range. The simulation results and experiments are found to be in very good agreement.

1. Introduction

Monte Carlo (MC) simulation methods require an accurate knowledge of the processes governing the penetration of positrons [1, 2] in matter. For energies up to 100 keV, elastic and inelastic scattering processes undergone by the positrons travelling in the solid target dominate. Modelling of the positron beam behaviour inside the material of interest depends on the reliability of the models describing these processes [3–12]. Knowledge of the collision processes, i.e. the scattering cross sections, can be used to find positron trajectories in an MC simulation. From the elastic differential cross sections (DCSs), the angular deflection distribution is calculated and used by random sampling to simulate the elastic events in chronological successions, i.e. true event-by-event MC simulation. In principle, this detailed simulation is exact when accurate DCSs are adopted [13]. However, in real simulations and for progressively higher energies of the incoming positrons, the number of scattering events per track increases gradually. In such cases (a few hundred keV and larger), detailed MC simulation is not practical.

Recently [14], we have elaborated an improved practical method to simulate elastic electron scattering in which single scattering events have been simulated using simple analytical expressions derived from the Wentzel model. We have shown that simulating with the Wentzel model reduces to a pure problem of optimization. In the present study, we have applied the

model for positrons. Our modelling, using the optimized Wentzel (OW2) model [14], yields an analytic expression convenient for MC calculations and reproduces values of the total elastic cross sections and the first and second transport cross sections obtained from partial wave (PW) calculations. The theoretical framework needed to derive the OW2 model is described first, followed by the simulation strategy used to test the validity of the model. In section 4, extensive comparisons with experiment and accurate MC models are made for both normal and oblique incidence. The advantages of the suggested model are discussed at the end of the paper.

2. Theoretical framework

Using the Wentzel model, i.e. using a simplified scattering potential in an exponential form to reproduce the effect of screening [15], the elastic DCS of a positron scattered by an atom is obtained in the first Born approximation as

$$\frac{\mathrm{d}\sigma^W(\theta)}{\mathrm{d}\theta} = \frac{\pi e^4}{2}\left(\frac{ZZ'}{E}\right)^2 \frac{\sin\theta}{(1-\cos\theta+\gamma)^2} \tag{1}$$

where γ represents the screening parameter ($\gamma = \frac{e^2}{4a_0}\frac{Z^{2/3}}{E}$).

The Wentzel total cross section σ_0^W is given as

$$\sigma_0^W = \int_0^\pi \frac{\mathrm{d}\sigma^W}{\mathrm{d}\theta}\,\mathrm{d}\theta = \frac{\pi e^4}{2}\left(\frac{ZZ'}{E}\right)^2 \frac{2}{\gamma(2+\gamma)}. \tag{2}$$

The Wentzel transport cross sections can be calculated analytically. In particular, the first and second transport cross sections σ_1^W and σ_2^W are expressed as

$$\sigma_1^W = \sigma_0^W\left[\frac{\gamma\,(\gamma+2)}{\gamma}\ln\left(\frac{\gamma+2}{\gamma}\right)-\gamma\right] \tag{3}$$

$$\sigma_2^W = \sigma_0^W\left[\frac{3\gamma}{2}\,(\gamma+1)\,(\gamma+2)\ln\left(\frac{\gamma+2}{\gamma}\right)-3\gamma\,(\gamma+2)\right]. \tag{4}$$

The probability $P(\theta)$ that a particle scatters by an angle θ is calculated from the distribution of the angular deflection as

$$P(\theta) = \frac{\int_0^\theta \frac{\mathrm{d}\sigma^W}{\mathrm{d}\theta'}\,\mathrm{d}\theta'}{\sigma_0^W} = \frac{(1+\gamma/2)(1-\cos\theta)}{(1+\gamma-\cos\theta)}. \tag{5}$$

Using equation (5), one can thus sample the scattering angle as

$$\cos\theta = 1 - \frac{2\gamma P(\theta)}{2+\gamma-2P(\theta)}. \tag{6}$$

It is important to note that equation (6) is very useful for MC simulations since it requires only the value of the screening parameter and a random value $P(\theta)$. In MC calculations, the random values $P(\theta)$ are represented by random numbers. However, the values of the screening parameter as described in the Wentzel model lead to inaccurate values of the Wentzel transport cross sections $\sigma_l^W(0, 1, 2, \ldots)$ at low and medium energies. It is well known that accurate values of $\mathrm{DCS}^{\mathrm{PW}}$ and σ_l^{PW} can be obtained from partial wave (PW) calculations or from suitable high-energy approximations [19]. Following the procedure in [14], we conclude again that the use of σ_l^{PW} ($l = 0, 1, 2$) as input in the system of equations (2), (3) and (4) leads to different values of the screening parameter γ since the solution is not unique. An example is given in figures 1(a) and (b), where we show that it is not possible to find a vector of values $\gamma(E)$ so as to reproduce exactly the values of the elastic cross sections calculated from the PW method. As a consequence, the optimization procedure (OW2) described in [14] based on the use of genetic

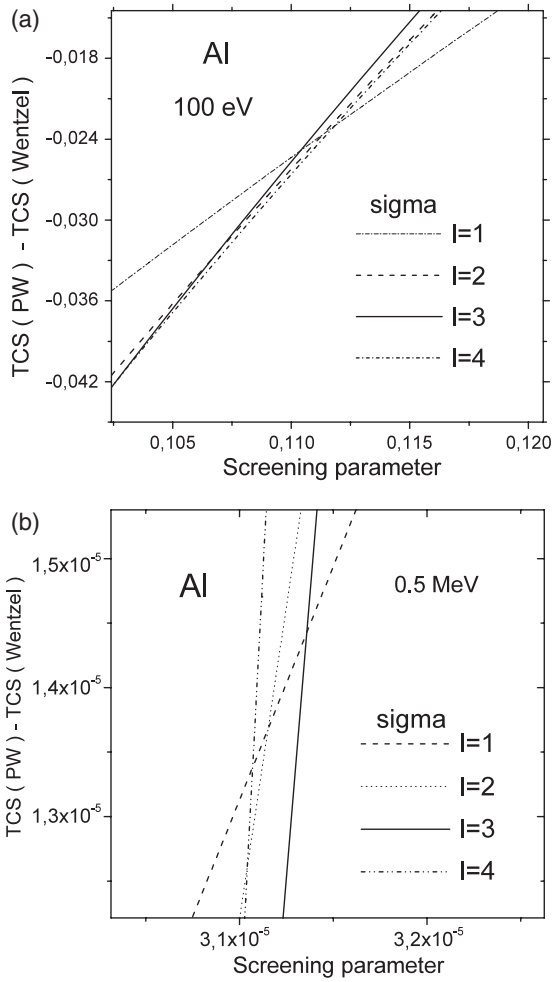

Figure 1. (a) Differences between Wentzel and PW transport cross sections of 100 eV positrons in Al. (b) Differences between Wentzel and PW transport cross sections of 0.5 MeV positrons in Al.

algorithms [16–18] is applied here for positrons. An example of results using the Wentzel model (OW2) for positrons energies up to 100 keV is presented in figure 2, where the total cross section and the first and second transport cross sections calculated for an Al target are presented. As a comparison, values of the PW calculations [19] are also represented.

3. Monte Carlo calculations

Backscattering coefficients for positrons impinging on solid targets may provide stringent tests on the accuracy of the description of the scattering processes. Calculations of positron backscattering coefficients as a function of both incident angles and target atomic number Z for a large range of energies have been made by several authors [4–12, 20, 21].

3.1. Elastic and inelastic processes

The elastic cross sections used in the optimized Wentzel model (OW2) are obtained using the Dirac PW analysis (ELESPA code) [19] for scattering by a local central interaction potential

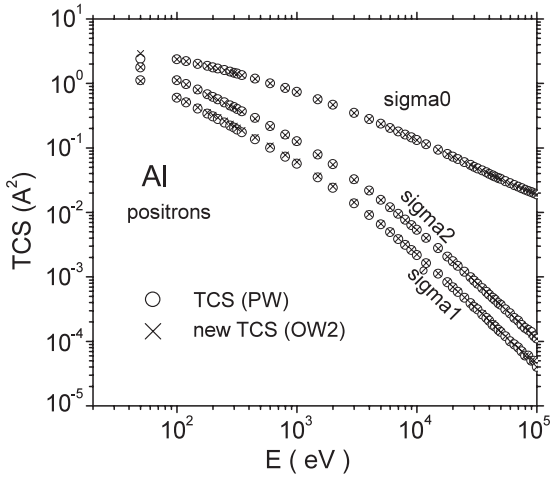

Figure 2. Transport cross sections ($l = 0, 1, 2$) calculated from the OW2 model. For comparison, transport cross sections calculated from the PW from ELESPA code [19] are also represented.

$V(r)$. In ELESPA, the potential is selected from four different electron density models, namely, the Thomas–Fermi–Molière (TFM), the Thomas–Fermi–Dirac (TFD), the Dirac–Hartree–Fock–Slater (DHFS) and the numerical densities obtained from multiconfiguration Dirac–Fock (DF) self-consistent calculations. In the present study, $V(r)$ is calculated using our numerical self-consistent electron densities calculated from density functional theory [22], where the calculations are performed self-consistently for each bound electron state of the atom within the local spin density approximation (LSDA) [23]. Exchange and correlation functional approximation and atomic configurations are used from [24] and [25], respectively. In these self-consistent calculations, atomic electron densities, Coulomb potentials, the energy eigenvalue, the integration of the radial Schrödinger equation and the screened Poisson integral are evaluated numerically using the Herman and Skillman calculations [25] on a radial mesh of 440 r-values. A comparison between the different electron density models cited before is shown in figures 3(a) and (b) for Cu and Ag. Good agreement is found between our calculated LSDA and DF electron densities which are both performed self-consistently. In figure 3(a) the Cu LSDA and DF electron densities are indistinguishable. The TFM, TFD, and DHFS electron densities are analytical models and can be used only as approximations.

When the atom is bound in a solid the interaction potential between the charged particle and the atom is different from that of the charged particle-free atom due to the crystalline structure, and hence solid-state effects should be included. The effect of the lattice structure is included in the elastic collision but channelling processes are excluded [26]. Solid-state effects have been introduced by using the muffin-tin model in which the potential of each atom of the solid is altered by the nearest neighbour [27–29].

The inelastic process is introduced in the present MC simulation by using a simple approximation to calculate the energy loss of the positron in which we assume that a positron loses its energy in a continuous manner between elastic collisions. Functions describing the energy loss are calculated using Gaussian quadrature of the polynomial best fits of the stopping power numerical results given by Ashley [30]. Values of Ashley's stopping powers for Al, Cu, Ag and Au are presented in figure 4.

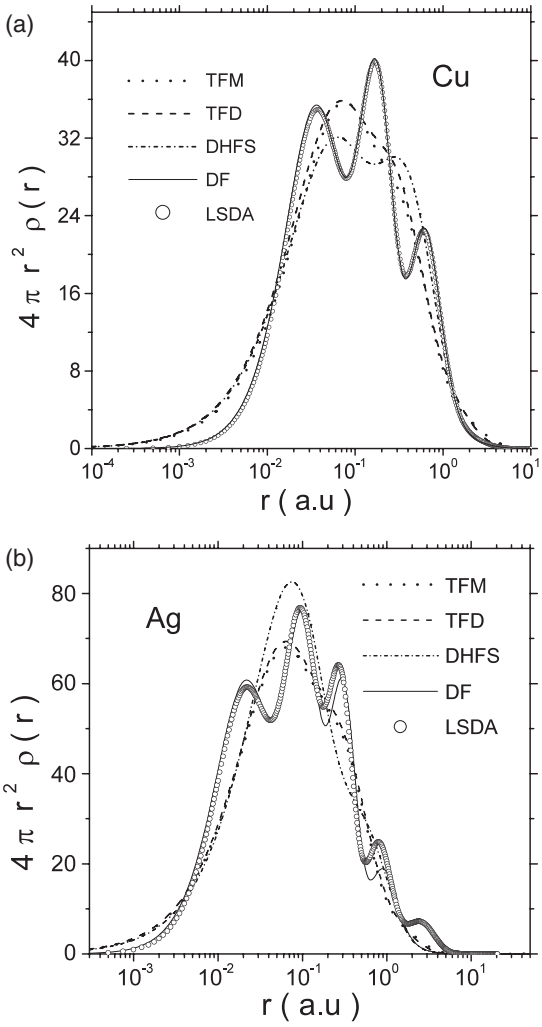

Figure 3. (a) Cu electron densities calculated from different models. (b) Ag electron densities calculated from different models.

3.2. Simulation procedure

The positron trajectories are constructed using the linear step lengths described by the exponential distribution as

$$P(s) = (1/\lambda_e)\exp(-S/\lambda_e) \tag{7}$$

where the distance S travelled between two elastic collisions is calculated by injecting a random number $R_1 \in (0-1)$ in equation (7) as

$$S = -\lambda_e \,\mathrm{Ln}\,(R_1). \tag{8}$$

The mean free path λ_e is calculated from the knowledge of the elastic cross section and the number of atoms per unit volume as

$$\lambda_e = (N\sigma_e^{PW})^{-1}. \tag{9}$$

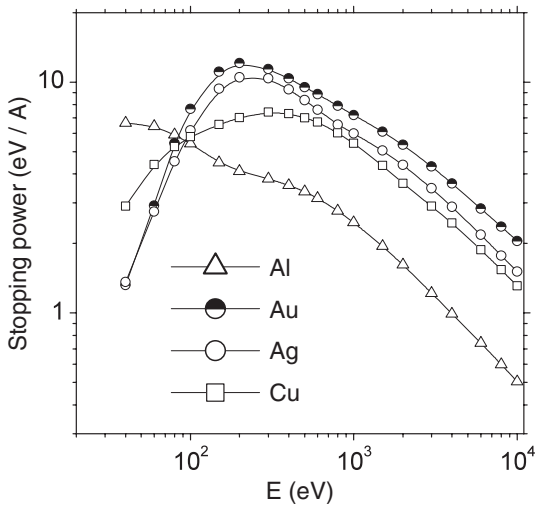

Figure 4. Ashley's stopping power of keV positrons for elemental solids Al, Cu, Ag, Au [29].

The energy loss ΔE along the distance S travelled between collisions is calculated as

$$\Delta E = \left(\frac{\mathrm{d}E}{\mathrm{d}S}\right) S. \tag{10}$$

The azimuthal angle is uniform between 0 and 2π and is defined by using a second random number R_2 as

$$\phi = 2\pi R_2. \tag{11}$$

The polar scattering angle after an elastic collision is calculated by injecting a third random number R_3 in equation (6) derived from the Wentzel model as

$$\theta = \mathrm{Arccos}\left(1 - \frac{2\gamma R_3}{2 + \gamma - 2R_3}\right) \tag{12}$$

where the screening parameter is a function of the energy calculated from the optimized Wentzel model (OW2). Values of $\gamma(E)$ for different elements in the keV range are shown in figures 5(a)–(c). Also represented are values of the elastic cross sections calculated from the PW model and those obtained from our resulting model (OW2).

4. Simulation results

The accuracy of the elastic process using our (OW2) model is tested in the present MC calculations by comparison of the calculated backscattering probabilities with experiment. The backscattering probability results represent a crucial test for the validity of any MC simulation.

Backscattering probabilities are calculated for keV and sub-keV positrons impinging with normal and oblique incidence on semi-infinite solids. Elemental solids varying from $Z = 13$ to 79 are considered. The termination energy considered is ~100 eV. Typically 10^5–10^6 positron trajectories are constructed in the present simulations.

Table 1 reports our MC results for the positron backscattering probabilities (referred to as Present MC) for various values of Z and for positron primary energy in the range 1–10 keV. For comparison, our recent theoretical backscattering coefficients [20], and experimental measurements of Coleman and MC simulations results of Jensen and Walker reported in [8] are also presented. Accordingly, there is a reasonable agreement between our results and the

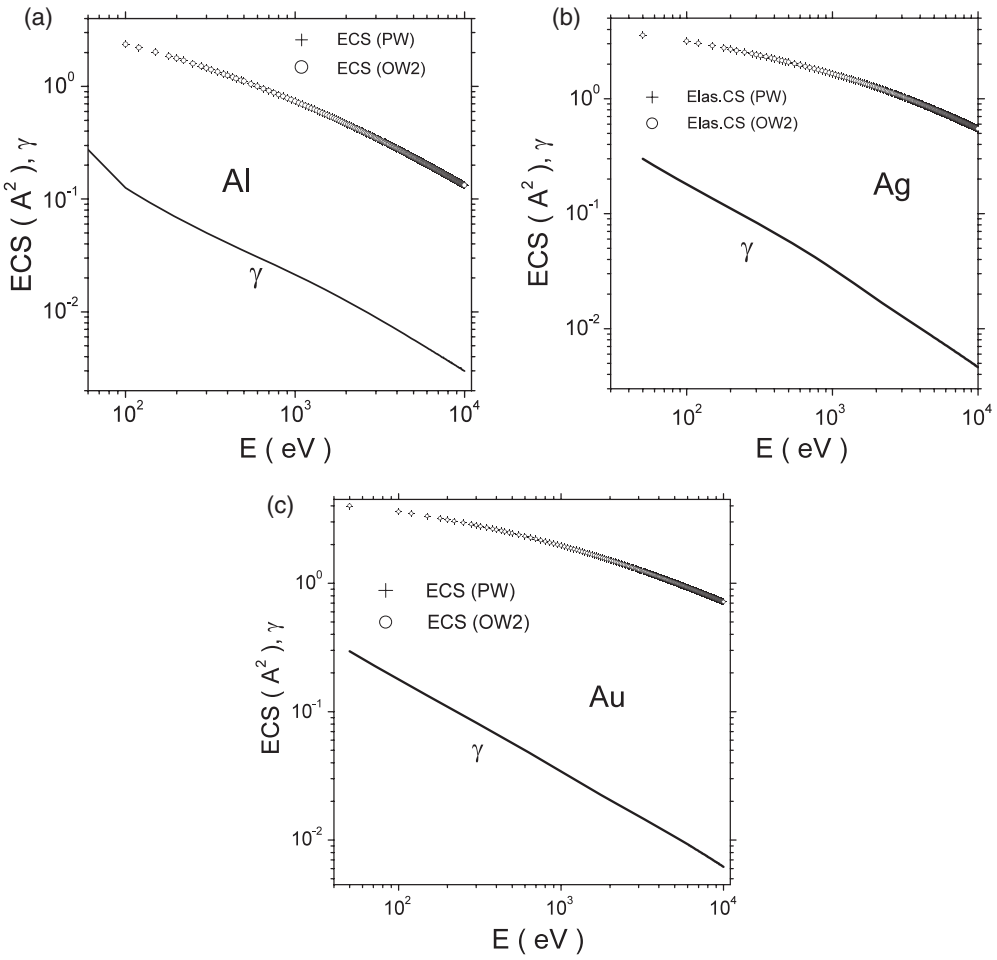

Figure 5. (a) Values of the screening parameter of Al using the OW2 model in the range 50–10 000 eV. Calculated elastic cross sections from the OW2 and PW models are also represented. (b) Values of the screening parameter of Ag using the OW2 model in the range 50–10 000 eV. Calculated elastic cross sections from the OW2 and PW models are also represented. (c) Values of the screening parameter of Au using the OW2 model in the range 50–10 000 eV. Calculated elastic cross sections from the OW2 and PW models are also represented.

available experimental ones. Moreover, our results are closer to experimental findings than those of the MC simulations. Note that in [4, 8], event-by-event MC calculation is considered. Numerical differential cross sections in scattering angle and in energy loss are used to calculate the angular deflection distribution and the energy loss distribution, respectively. The elastic model has been modelled using partial wave calculations and the inelastic process using the full Penn model [4].

In [20], we used a theoretical model [31] derived from the transport equation of Boltzman with accurate transport cross sections as well as Ashley's stopping power functions, making the calculation of the backscattering coefficients less time consuming and in better agreement with experiment. However, the calculated theoretical backscattering coefficients are in closer agreement with experiment than the MC calculations, as suspected by transport theory.

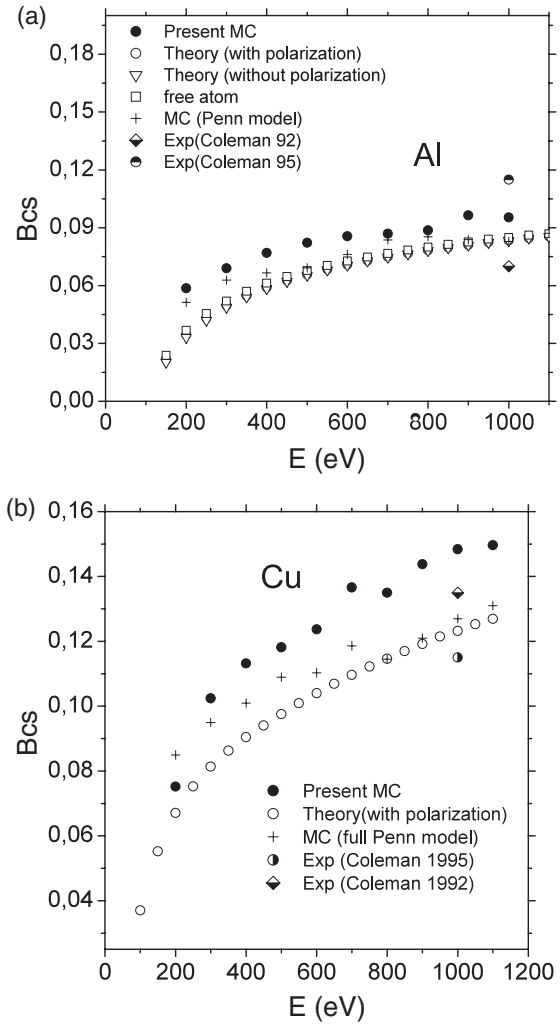

Figure 6. (a) Low-energy positron backscattering results from Al calculated using different models [21]. (b) Low-energy positron backscattering results from Cu calculated using different models [21].

For oblique incidence, few experimental data exist. Meanwhile, as an example of illustration, in table 2 we have compared our results to the experimental backscattering coefficients reported in [8] of 5 keV positrons impinging on Al and Au as light and heavy element with oblique incidence θ varying in the range $0° \leqslant \theta \leqslant 80°$, respectively. The agreement found reinforces the validity of our modelling to the elastic process using the optimized Wentzel model (OW2).

Results for the backscattering probabilities and coefficients in the sub-keV range (100–1000 eV) have been published and discussed in detail recently in [21].

In particular, the shape of the backscattering coefficient curves calculated for materials with different Z has been studied, showing a different behaviour from that in the keV range as Z increases.

Sub-keV backscattering results are shown in figure 6(a), (b) for Al and Cu, respectively. For comparison, different sets of data calculated with different methods as described before are plotted. Also, the measurements of Coleman at 1 keV of 1992 [8] and 1996 [32] are added. Particular attention has been focused in [21] on the polarization and solid-state effects. We have

Table 1. Calculated (Present (OW2)), theoretical (Theo) [20], experimental (Exp) [8] and MC simulation (MC) [8] results for positron (E = 1–10 keV) backscattering coefficients from Al, Cu, Ag and Au.

Z	E (keV)	1	2	3	4	5	6	7	8	9	10
	Present (OW2)	0.0954	0.0978	0.0981	0.0960	0.0989	0.0992	0.100	0.104	0.105	0.109
	Theo [20]	0.0864	0.0987	0.104	0.107	0.111	0.113	0.116	0.118	0.120	0.123
13	Exp [8]	0.069	—	0.086	—	0.112	—	0.122	—	—	0.123
	MC [8]	0.109	—	0.115	—	0.126	—	0.125	—	—	0.128
	Present (OW2)	0.148	0.169	0.178	0.188	0.194	0.199	0.208	0.210	0.214	0.218
	Theo [20]	0.117	0.146	0.163	0.175	0.185	0.193	0.200	0.205	0.210	0.215
29	Exp [8]	0.135	—	0.177	—	0.205	—	0.226	—	—	0.229
	MC [8]	0.156	—	0.194	—	0.205	—	0.231	—	—	0.235
	Present (OW2)	0.131	0.154	0.177	0.198	0.2156	0.230	0.241	0.255	0.264	0.278
	Theo [20]	0.109	0.146	0.173	0.194	0.212	0.228	0.242	0.254	0.266	0.277
47	Exp [8]	0.106	—	0.168	—	0.227	—	0.243	—	—	0.277
	MC [8]	0.126	—	0.182	—	0.216	—	0.236	—	—	0.245
	Present (OW2)	0.128	0.161	0.189	0.207	0.226	0.240	0.251	0.263	0.273	0.276
	Theo [20]	0.112	0.153	0.182	0.205	0.223	0.239	0.252	0.264	0.275	0.285
79	Exp [8]	0.123	—	0.186	—	0.232	—	0.273	—	—	0.294
	MC [8]	0.168	—	0.242	—	0.290	—	0.316	—	—	0.340

Table 2. Calculated (Present (OW2)), theoretical (Theo) [20], experimental (Exp) [8] and MC simulation (MC) [8] results for 5 keV positron backscattering coefficients from Al and Au versus angle of incidence.

	θ (deg)	0	10	20	30	40	50	55	60	65	70	80
	Present (OW2)	0.0989	0.101	0.113	0.138	0.172	0.228	0.266	0.313	0.370	0.425	0.583
	Theo [20]	0.111	0.114	0.124	0.143	0.177	0.237	0.281	0.341	0.419	0.517	0.754
13	Exp [8]	0.112	0.113	0.110	0.116	0.141	0.166	—	0.240	—	—	—
	MC [8]	0.126	0.134	0.143	0.167	0.203	0.254	—	0.334	—	0.443	0.568
	Present (OW2)	0.226	0.231	0.243	0.270	0.312	0.369	0.401	0.443	0.488	0.537	0.670
	Theo [20]	0.223	0.230	0.246	0.278	0.331	0.412	0.465	0.528	0.599	0.676	0.836
79	Exp [8]	0.232	0.256	0.247	0.256	0.326	0.426	0.468	—	0.553	—	—
	MC [8]	0.290	0.295	0.301	0.336	0.369	0.422	—	0.478	—	0.552	0.673

shown that for energies up to 800 eV, polarization and solid-state effects should be included in the transport of positrons.

We consider the backscattering calculations presented in figure 6(a), (b) as predictive results since to our knowledge no experimental data exist in this range. However, they agree both in shape and in the range of results.

5. Discussion

The elastic process plays a central role in the transport of charged particles in matter. We have presented a simplified model for positrons derived from the Wentzel model to be used with ease in a Monte Carlo code. We have shown that the Wentzel model could not be used directly as an equivalent model of the numerical partial wave calculations but only with an optimized procedure. The validity of our model has been discussed for the simple but important case of keV positrons since it represents the range of the non-applicability of Wentzel model.

Indeed, the resulting optimized model (OW2) has been tested after being implemented in a simple 'CSDA' Monte Carlo code to calculate the backscattering probabilities from four elemental solids with Z varying from 13 to 79 in the keV range. The results have been found to be in agreement with the measurements of Coleman *et al* [8] for both normal and oblique incidence. Thus, as a conclusion, we suggest the use of our optimized Wentzel (OW2) elastic model for general purposes in surface science and related applications based on Monte Carlo simulations. The OW2 model has the advantages of avoiding the use of the large memory space of numerical differential cross sections by using one vector $\gamma(E)$ for each element and of considerably reducing the time taken for the simulation since a simple analytic expression for the sampling of the angular deflection is used.

Finally, it is important to note that the present Monte Carlo simulation is based on the continuous slowing down approximation, and thus could be used to calculate backscattering, absorption and transmitted probabilities and other physical quantities related to the trajectories of the positrons but not the individual energy loss during the slowing down. Similar work taking into account the fluctuations in energy loss is under construction. Results will be given in the near future.

References

[1] See reviews by Lynn K G and McKee T A 1979 *J. Appl. Phys.* **19** 247
Mills A P Jr 1979 *Appl. Phys. Lett.* **35** 427
[2] Schultz P J and Lynn K G 1988 *Rev. Mod. Phys.* **60** 701
[3] Massoumi G R, Hozhabri N, Jensen K O, Lennard W N, Lorenzo M S, Schultz P J and Walker A B 1992 *Phys. Rev. Lett.* **68** 3873
[4] Jensen K O and Walker A B 1993 *Surf. Sci.* **292** 83
[5] Fernandez-Varea J M, Liljequist D, Csillag S, Räty R and Salvat F 1996 *Nucl. Instrum. Methods* B **108** 35
[6] Aers G C 1994 *Appl. Phys. Lett.* **64** 661
[7] Massoumi G R, Lennard W N, Schultz P J, Walker A B and Jensen K O 1993 *Phys. Rev.* B **47** 11007
[8] Coleman P G, Albrecht L, Jensen K O and Walker A B 1992 *J. Phys.: Condens. Matter* **4** 10311
[9] Baker J A, Chilton N B, Jensen K O, Walker A B and Coleman P G 1991 *J. Phys.: Condens. Matter* **3** 4109
[10] Ghosh V J and Aers G C 1995 *Phys. Rev.* B **51** 45
[11] Dapor M 1995 *J. Appl. Phys.* **77** 2840
[12] Dapor M 2004 *Phys. Lett.* A **333** 457
[13] Benedito E, Fernadez-varea J M and Salvat F 2001 *Nucl. Instrum. Methods* B **174** 91
[14] Chaoui Z 2006 *Appl. Phys. Lett.* **88** 024105
[15] Wentzel G 1927 *Z. Phys.* **40** 590
[16] Hill R R 1999 *Proc. 1999 Winter Simulation Conf.* ed P A Farrington, H B Nembhad, D T Sturrock and G W Evans (New Jersey: Prentice-Hall) p 543
[17] Zeiri Y, Fattal E and Kosloff R 1995 *J. Chem. Phys.* **102** 1859
[18] Luo Y H, Zhao J, Qiu S and Wang G 1999 *Phys. Rev.* B **59** 14903
[19] Salvat F, Jablonski A and Powell C J 2005 *Comput. Phys. Commun.* **165** 157
[20] Chaoui Z and Bouarissa N 2004 *J. Phys.: Condens. Matter* **16** 718
[21] Chaoui Z 2006 *Appl. Surf. Sci.* **252** 3362
[22] Hohenberg P and Kohn W 1964 *Phys. Rev.* B **136** 864
Kohn W and Sham L J 1965 *Phys. Rev.* A **140** 1133
[23] Gunnarsson O and Lundqvist B I 1976 *Phys. Rev.* B **13** 4274
[24] Perdew J P and Wang Y 1992 *Phys. Rev.* B **45** 13244
[25] Herman F and Skillman S 1963 *Atomic Structure Calculations* (New Jersey: Prentice-Hall)
[26] Niedrig H 1982 *J. Appl. Phys.* **53** 4
[27] Salvat F and Mayol R 1993 *Comput. Phys. Commun.* **74** 358
[28] Czyzewsk Z, O'Neill D, MacCallum C J, Romig A and Joy D C 1990 *J. Appl. Phys.* **68** 3066
[29] Chaoui Z and Bouarissa N 2004 *J. Appl. Phys.* **96** 1 807
[30] Ashley J C 1990 *J. Electron. Spectrosc. Relat. Phenom.* **50** 323
[31] Vicanek M and Urbassek H M 1991 *Phys. Rev.* B **44** 7234
[32] Knights A P and Coleman P G 1995 *J. Phys.: Condens. Matter* **7** 3485